Received: 22 October 2019 | Revised: 11 March 2021 | Accepted: 12 April 2021

DOI: 10.1002/ldr.3968

RESEARCH ARTICLE

WILEY

Tillage erosion as an important driver of in-field biomass patterns in an intensively used hummocky landscape

Lena Katharina Öttl[1] | Florian Wilken[1,2] | Karl Auerswald[3] | Michael Sommer[4,5] | Marc Wehrhan[4] | Peter Fiener[1]

[1]Working Group Water and Soil Resource Research, Institute of Geography, University of Augsburg, Augsburg, Germany

[2]Department of Environmental Systems Science, ETH Zürich, Zürich, Switzerland

[3]Aquatic Systems Biology Unit, Technical University of Munich, Munich, Germany

[4]"Landscape Pedology" Working Group, Leibniz Centre for Agricultural Landscape Research ZALF e.V., Müncheberg, Germany

[5]Institute of Environmental Science and Geography, University of Potsdam, Potsdam, Germany

Correspondence
Peter Fiener, Alter Postweg 118, 86159 Augsburg, Germany.
Email: fiener@geo.uni-augsburg.de

Funding information
Deutsche Forschungsgemeinschaft, Grant/Award Numbers: FI-1216/12-1, SO-302/12-1

Abstract

Tillage erosion causes substantial soil redistribution that can exceed water erosion especially in hummocky landscapes under highly mechanized large field agriculture. Consequently, truncated soil profiles can be found on hill shoulders and top slopes, whereas colluvial material is accumulated at footslopes, in depressions, and along downslope field borders. We tested the hypothesis that soil erosion substantially affects in-field patterns of the enhanced vegetation index (EVI) of different crop types on landscape scale. The interrelation between the EVI (RAPIDEYE satellite data; 5 m spatial resolution) as a proxy for crop biomass and modeled total soil erosion (tillage and water erosion modeled using SPEROS-C) was analyzed for the Quillow catchment (size: 196 km^2) in Northeast Germany in a wet versus normal year for four crop types (winter wheat, maize, winter rapeseed, winter barley). Our findings clearly indicate that eroded areas had the lowest EVI values, while the highest EVI values were found in depositional areas. The differences in the EVI between erosional and depositional sites are more pronounced in the analyzed normal year. The net effect of total erosion on the EVI compared to areas without pronounced erosion or deposition ranged from −10.2% for maize in the normal year to +3.7% for winter barley in the wet year. Tillage erosion has been identified as an important driver of soil degradation affecting in-field crop biomass patterns in a hummocky ground moraine landscape. While soil erosion estimates are to be made, more attention should be given toward tillage erosion.

KEYWORDS
agroscapelab Quillow, crop biomass patterns, EVI, remote sensing, tillage erosion

1 | INTRODUCTION

Soil erosion on arable land is one of the most destructive human perturbations to soil sustainability and food security (Amundson et al., 2015; Zhao et al., 2018). The effect of soil erosion on crop biomass and yields was investigated in a large number of studies (Bakker, Govers, & Rounsevell, 2004) that showed a wide range of yield reduction (Den Biggelaar, Lal, Wiebe, & Breneman, 2003). Even if the different experimental setups make it difficult to compare the results of different studies, more or less standardized desurfacing

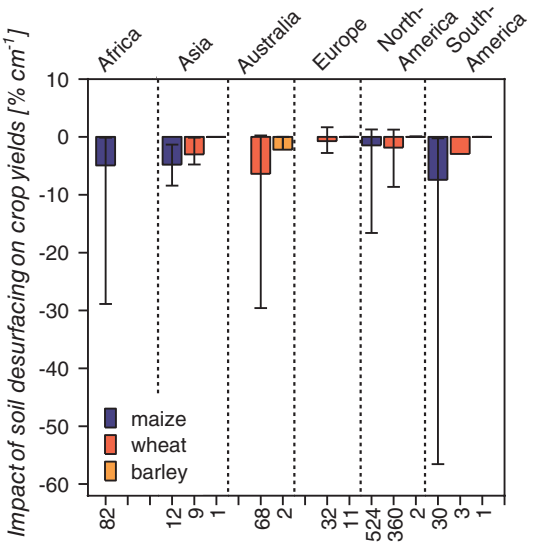

FIGURE 1 Impact of desurfacing on maize, wheat, and barley yields. Data from different continents. Erosion-induced yield effects were calculated relative to the yield of all treatments of the single experiments (18 to 30 cm of topsoil removed) following the methodology of Den Biggelaar et al. (2003). Numbers at x-axis indicate the number of records taken into account for each crop type per continent respectively. Data are taken from the review of Den Biggelaar et al. (2003) and expanded with data from a variety of sources (Allen et al., 2011; Gorji et al., 2008; Izaurralde et al., 2006; Larney, Janzen, Olson, & Olson, 2009; Sui et al., 2009) [Colour figure can be viewed at wileyonlinelibrary.com]

experiments from different continents underline the general tendency that eroded soils lose crop yield potential (Figure 1). As most of these artificial experiments were performed on soils without substantial (pre-)erosion, the reduction in crop yields would be even more pronounced in landscapes strongly affected by erosion at the beginning of such experiments.

The decline in yields at eroded soils can be mainly traced back to a reduction in soil depth and corresponding rooting depth, a reduction in nutrient availability and storage potential, and changes in soil physical properties like porosity, infiltration capacity, and water holding capacity (Den Biggelaar, Lal, Wiebe, & Breneman, 2001; Herbrich, Gerke, & Sommer, 2018; Lal, Mokma, & Lowery, 1999; Quinton, Govers, Van Oost, & Bardgett, 2010). In contrast to the decrease in yields at eroding sites, the potential increase in yields at depositional sites is less intensively studied. However, several studies indicate that crop yields at depositional sites exceed those at erosional sites (Heckrath et al., 2005; Papiernik et al., 2005; Wehrhan, Rauneker, & Sommer, 2016).

In general, tillage leads to a truncation of soil profiles at convexities or upslope field borders, which results in shallower soils and subsequently in an incorporation of subsoil or parent material with poorer physical or chemical properties (De Alba, Lindstrom, Schumacher, & Malo, 2004; Gerke & Hierold, 2012). Moreover, subsoil of higher bulk density and missing continuous pore space can be a barrier for root growth (Chirinda et al., 2014; Herbrich et al., 2018; Singh, Choudhary, Singh, Singh, & Mishra, 2019) and, therefore, reduce water and nutrient accessibility. Modified soil properties (e.g., soil organic carbon, clay content, soil moisture) at erosional sites show the strongest effect on crop yields during dry years (Chi, Bing, Walley, & Yates, 2009; Den Biggelaar et al., 2001; Kravchenko, Robertson, Thelen, & Harwood, 2005), resulting in a more pronounced in-field variation of crop growth and yields (Stadler et al., 2015; Taylor, Wood, Earl, & Godwin, 2003). The decline of yields at erosional sites is smaller or may even disappear in wet years, as water limitations are less important. In very wet years, yields at erosional sites may exceed those at depositional sites as high groundwater level and resulting oxygen deficiency in closed depressions and lower landscape positions will negatively affect crop growth conditions at depositional sites (Gerke, Rieckh, & Sommer, 2016; Kaspar et al., 2004; Martinez-Feria & Basso, 2020). However, this is not or only indirectly related to soil redistribution processes.

Although tillage-induced soil redistribution globally occurs in many areas, its deteriorating effect on soil properties especially affects areas with short summit-footslope distances and relatively shallow soils, which are faced with decreasing yields at hilltops. This has been recognized for the hummocky young moraine landscapes of North America (Papiernik et al., 2005; Pennock, 2003; Thaler, Larsen, & Yu, 2021), northern Europe (Heckrath et al., 2005), and Russia (Olson, Gennadiyev, Jones, & Chernyanskii, 2002).

Considering different erosion types, tillage erosion is still understudied compared to water and wind erosion (Fiener et al., 2018), although their rates are often in the same order of magnitude or even exceed those of other erosion types (Govers, Quine, Desmet, & Walling, 1996; Lobb, Kachanoski, & Miller, 1995; Schimmack, Auerswald, & Bunzl, 2002). Nevertheless, their spatial patterns are quite different: Tillage erosion exclusively leads to in-field soil redistribution without off-site damage (Van Oost, Govers, De Alba, & Quine, 2006). Thereby, soil loss by tillage often occurs at landscape positions where water erosion is minimal (at convexities, e.g., hilltops and slope shoulders), while soil accumulation by tillage takes place at positions where water erosion is maximal (in concavities, especially along drainage ways where overland flow concentrates) (Govers, Lobb, & Quine, 1999). Moreover, tillage erosion patterns are dominated by the field layouts with highest erosion at the upslope field borders and most deposition at the downslope field borders (Wilken, Sommer, Van Oost, Bens, & Fiener, 2017).

Compared to the large number of studies assessing the effect of erosion on field-scale crop yields (e.g., Lal, Ahmadi, & Bajracharya, 2000; Larney et al., 2009), there are only few studies investigating a larger landscape scale (e.g., Battiston, Miller, & Shelton, 1987; Thaler et al., 2021). For example, in the young morainic landscape of Ontario, Canada (study area: 90 km^2), moderate to severely eroded soils (water and wind erosion) led to an average decline in maize yield of ca. 3.6%, whereby the redistribution and deposition of the eroded material were not considered (Battiston et al., 1987). In the morainic landscape of the midwestern United States ('Corn Belt region'; study area: 210 km^2), an annual crop yield reduction of 6 ± 2% due to A-horizon loss was found, which was mainly traced back to tillage erosion (Thaler et al., 2021). However, soil redistribution as a combination of erosion and deposition was not

considered, although it is highly relevant for landscape-scale understanding of yield patterns as the negative effects of soil erosion may be partly compensated by positive effects at depositional sites (Govers, Poesen, & Goossens, 2004).

For the comparison of the erosion and biomass patterns on landscape scale, remote sensing products are required that provide a relatively high spatial resolution (< 10 m) (Wehrhan et al., 2016) and spectral bands that are suitable for crop biomass detection (red and near infrared, NIR) (Gao, Huete, Ni, & Miura, 2000). Therefore, the spectral properties should be suitable for a rather linear representation of low and high biomass conditions (Huete et al., 2002). The enhanced vegetation index (EVI) has been developed to optimize the sensitivity for the reflectance of high, green biomass and to reduce soil background and atmospheric influences (Huete, Liu, Batchily, & Van Leeuwen, 1997). Imagery delivered by the RAPIDEYE satellite constellation (5 m spatial resolution; 5.5 day repetition cycle; 5 bands VIS–NIR) (Chander et al., 2013) has been proven to be useful for assessing crop variability (Reichenau et al., 2016; Shang et al., 2015) or to quantify vegetation cover (Rudolph et al., 2015; Shang et al., 2014).

To our knowledge, an investigation of the influence of soil redistribution on crop biomass on landscape scale in Europe has been little documented, although the young moraine landscape of central Europe is highly affected by combined tillage and water erosion (hereinafter referred to as total erosion) (Heinrich et al., 2018). In general, soils in loamy ground moraine landscapes are quite fertile (Sommer, Gerke, & Deumlich, 2008) and comprise important crop growth areas. Those soils that developed from glacial till are characterized by relatively shallow development depths compared to the mostly studied water-erosion prone loess areas and, thus, are more susceptible to a reduction in crop biomass production.

The aims of our study are (a) to compare spatial patterns of modeled tillage and water erosion against the EVI in an intensively used hummocky landscape of Northeast Germany, (b) to analyze the impact of soil redistribution on the EVI depending on crop type and differences in seasonal precipitation, and (c) determine the net effect of total soil redistribution on landscape-scale EVI as a proxy for crop biomass.

2 | MATERIALS AND METHODS

2.1 | Study site

The study area is located at ZALF's landscape laboratory 'AgroScapeLab Quillow', which comprises a catchment of approximately 196 km^2 located about 100 km north of Berlin, Germany (Figure 2). It represents a typical ground moraine landscape formed after the retreat of the Weichselian glaciers (ca. 15 ka BP) in Northeast Germany (shaded area in Figure 2) (Lüthgens, Böse, & Preusser, 2011). The hummocky area is characterized by a hilly topography with short summit-footslope distances (on average 35 m). Typical for the landscape is the large number of kettle holes, which were formed by melting of dead ice (Anderson, 1998) and only drain via sub-surface flow. These kettle holes can still be filled by water or (degraded) peat. However, many of them are nowadays covered by colluvial material, which resulted from centennial land use as arable land (Van der Meij et al., 2019). The 'AgroScapeLab Quillow' is not a typical catchment in a hydrological sense as a large part of the catchment drains into kettle holes, which are only connected to the River Quillow via complex groundwater fluxes (Lischeid et al., 2017). The mean slope (± standard deviation) of the study area is about 7% (± 6%) with a general west–east elevation gradient (from 165 to 15 m a.s.l.).

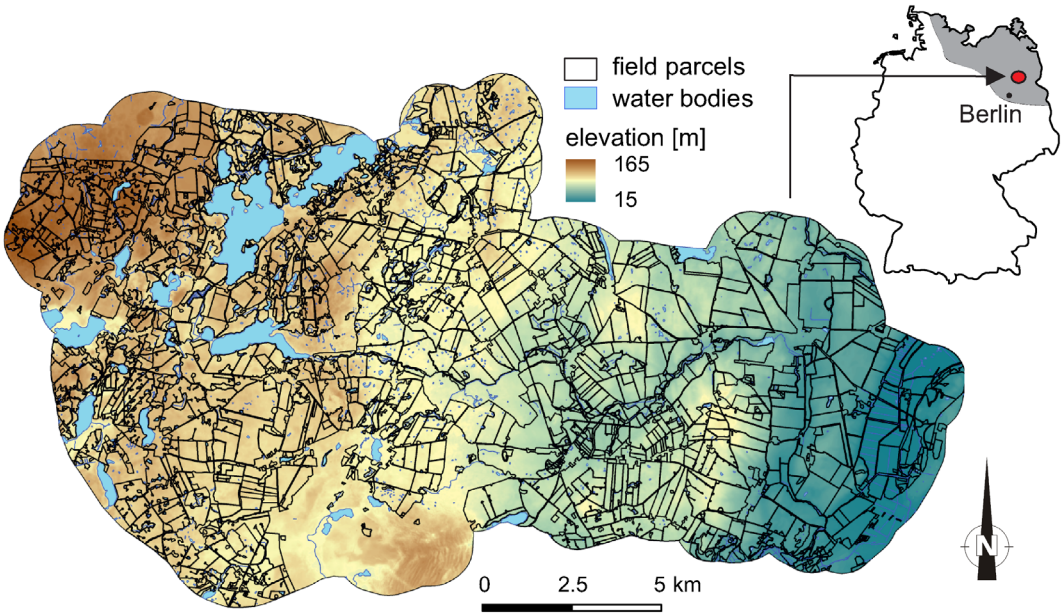

FIGURE 2 The study area 'AgroScapeLab Quillow' is located north of Berlin in the young moraine landscape of Northeast Germany (grey area of inset map) [Colour figure can be viewed at wileyonlinelibrary.com]

Land cover in this area is dominated by arable land and pasture (ca. 70%), followed by wetlands and lakes (ca. 16%), forest (ca. 11%), and settlements (ca. 3%) (Heinrich et al., 2018). Due to its fertile soils, large parts of the catchment are used for agricultural production since Neolithic times (Kappler et al., 2018; Sommer et al., 2008). Since the second half of the 20th century, agriculture was intensively mechanized and field sizes were substantially enlarged during the socialistic era of the German Democratic Republic (Bayerl, 2006). Today, the average field size is about 22 ha ± 20 ha (2–150 ha). Typical crop types are winter wheat (*Triticum aestivum* L.), winter barley (*Hordeum vulgare* L.), winter rapeseed (*Brassica napus* L.), and maize (*Zea mays* L.). The catchment is characterized by a subcontinental climate with an average annual air temperature of 9.3°C and a mean annual precipitation of 468 mm (20-year average 1999–2018, DWD meteorological station at Grünow). The average precipitation during the main growing season for wheat and maize is approximately 284 mm (April to September 1999–2018) (DWD Climate Data Center [CDC], 2018a, 2018b).

The soil pattern of the region (Figure 3) is related to topography and the heterogeneity of Pleistocene deposits and has been strongly modified by soil erosion over the past centuries (Deumlich, Schmidt, & Sommer, 2010; Koszinski, Gerke, Hierold, & Sommer, 2013; Sommer et al., 2008). Recently, only 20% of the arable land shows noneroded soils (Calcic Luvisols) (IUSS Working Group WRB, 2015), mainly at lower midslopes or flat plateaus. Extremely eroded soils (Calcaric Regosols) occur at hilltops, ridges, and slope shoulders, while strongly eroded soils (Nudiargic Luvisols) reach from slope shoulders to upper midslopes. Footslopes and closed depressions also comprise approximately 20% of the landscape. Here, groundwater-influenced colluvial soils (Gleyic-Colluvic Regosols, often overlying peat) have developed. Generally, the soil landscape reveals strong local gradients in wetness (<100 m distance), and the soil texture ranges from loamy sand (80% sand, 15% silt, 5% clay) to sandy clay loam (50% sand, 30% silt, 20% clay).

2.2 | Patterns of crop-specific EVI/biomass variability

RAPIDEYE satellite images were used to classify crop types and to determine in-field patterns of crop-specific EVI. The RAPIDEYE satellite system consists of five identical satellites and provides 5-band multispectral images on a basis of 5.5 days (at nadir) with a ground sample distance of 6.5 m. The five bands are visible blue (440–510 nm), green (520–590 nm), red (630–685 nm), red edge (690–730 nm), and near infrared (760–850 nm) (Chander et al., 2013; Planet, 2016). In this study, the Level 3A product was used, which is radiometrically and geometrically sensor corrected and resampled to 5 m spatial resolution (Chander et al., 2013). The advantages of the RapidEye satellite images are the relatively high spatial resolution, the short revisiting time, and the band-combination that is well suited for crop detection (Kim & Yeom, 2012).

Preprocessing of the RAPIDEYE imagery included atmospheric correction with the algorithm FLAASH (fast line-of-sight atmospheric analysis of spectral hypercubes; Cooley et al., 2002) of the software ENVI. Three cloud-free images in 2010 and 2015 (DOY (day of year) 2010: 168, 192, 266; DOY 2015: 155, 188, 262) were classified in a multitemporal maximum-likelihood approach with ERDAS Imagine to derive main crop types for further analysis (producer's accuracy in both years > 92.9%; user's accuracy > 86.4%) (ERDAS Inc., 2008; Tso & Mather, 2009). The four main crops used for further analysis accounted for approximately 80% of the arable land in both years. Their proportions in the year 2010(2015) were 38(36)% winter wheat, 21(18)% winter rapeseed, 11(14)% maize, and 8(9)% winter barley. The remaining area was covered by grassland, sugar beet (*Beta vulgaris* L.), and triticale (x *Triticosecale*) that are not further considered in this study.

To calculate the EVI of winter wheat, winter rapeseed, and maize, the July images from 2010 and 2015 were used (DOY 2010: 192, DOY 2015: 188). For winter barley, the June images were used

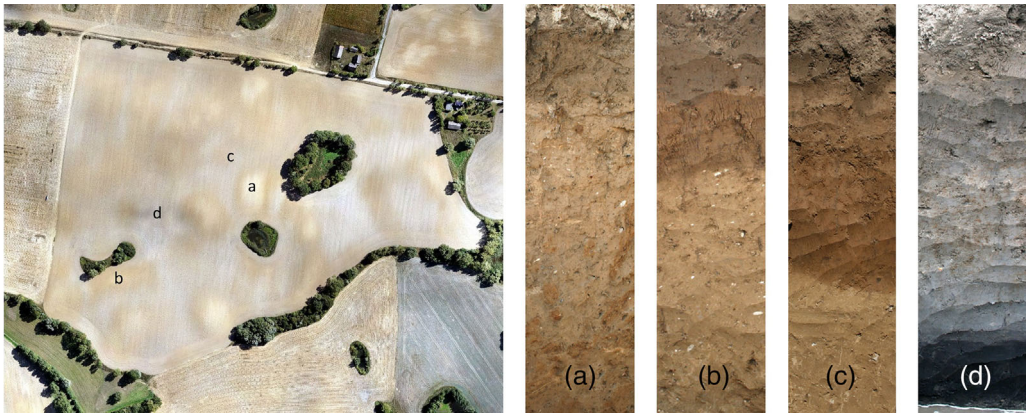

FIGURE 3 Erosion-affected soil pattern in the study area and corresponding exemplary soil profiles: Light colours at top slopes and hill shoulders indicate extremely eroded soils (a: Calcaric Regosols) by tillage erosion; brownish colours represent strongly eroded soils (b: Nudiargic Luvisols) affected by tillage and water erosion; brighter colours at lower midslopes indicate noneroded soils (c: Calcic Luvisols) and dark greyish areas indicate colluvial soils in closed depressions (d: Gleyic-Colluvic Regosols). Soil classification is according to IUSS Working Group WRB (2015) [Colour figure can be viewed at wileyonlinelibrary.com]

(DOY 2010: 169, DOY 2015: 155) because it was already partly harvested in July. Both years exhibited a similar overall precipitation before and during the growing season (November 2009–July 2010:323 mm; November 2014–July 2015:266 mm; DWD meteorological station at Grünow). However, there was a distinct difference in precipitation in the main growing season of the winter crops and maize (April–September; 405 mm in 2010; 211 mm in 2015) (DWD Climate Data Center [CDC], 2018b), which had a substantial effect on crop biomass production in those years. Hence, we further refer to 2010 as a wet year and 2015 as a normal year, respectively.

The use of the EVI is preferred over the most commonly used vegetation index, namely the normalized difference vegetation index (NDVI), for two reasons: The EVI was found to be a good indicator for crop biomass (Jin et al., 2017; Wehrhan et al., 2016) and is more sensitive to high biomass than the NDVI (Huete et al., 2002; Matsushita, Yang, Chen, Onda, & Qiu, 2007). The calculation of the EVI (range from 0 'no vegetation vitality' to 1 'very high vegetation vitality') is shown in Equation 1 (Huete et al., 1997, 2002).

$$\mathrm{EVI} = G \cdot \frac{(\mathrm{NIR} - R)}{(\mathrm{NIR} + C_1 \cdot R - C_2 \cdot B + L)} \quad (1)$$

Where: atmospherically corrected reflectance in the near infrared (NIR), red (*R*) and blue (*B*) spectral regions are combined. A gain factor ($G = 2.5$) and empirically derived correction factors are included to remove the soil signal from the mixed soil-vegetation spectral signature ($L = 1.0$) and atmospheric effects ($C_1 = 6.0$ and $C_2 = 7.5$) (Huete et al., 1997, 2002). As we did not carry out any biomass harvesting during the satellite overpasses, the EVI is used as a relative proxy variable for crop biomass.

The EVI was standardized to the mean and standard deviation of each agricultural field to remove the mean differences between fields and focus on in-field EVI variability (Equation 2).

$$\mathrm{EVI}_z = \frac{\mathrm{EVI}_i - \mathrm{mean}\left(\sum_{i=1}^{n} \mathrm{EVI}\right)}{sd\left(\sum_{i=1}^{n} \mathrm{EVI}\right)} \quad (2)$$

Where: the standardized EVI (EVI_z) is the difference of the EVI per grid cell *i* and the mean EVI of the grid cells *n* of the corresponding agricultural field divided by the standard deviation of the *n* EVI values of this field. All spatial analyses were performed using R version 3.6.1 (R Core Team, 2019) and ESRI ARCMAP version 10.5.1 (ESRI, 2017).

2.3 | Patterns of soil erosion

To determine soil erosion patterns, we used the well-established soil erosion and carbon turnover model SPEROS-C that allows calculating spatially explicit soil redistribution due to tillage and water in an annual time-step (Van Oost, Quine, Govers, & Heckrath, 2006). It is important to note here that we focus on the actual erosion pattern and not on the quantification of long-term soil loss or gain due to centuries of erosion. Hence, the underlying assumption is that this pattern is a good proxy for soil erosion and deposition in a region, which is under arable use for at least 500 years (Kappler et al., 2018; Sommer et al., 2008).

The tillage erosion pattern was calculated based on a diffusion-type equation developed by Govers, Vandaele, Desmet, Poesen, & Bunte (1994) (Equation 3). The net flux due to tillage (Q_{til}) can be written as

$$Q_{\mathrm{til}} = -k_{\mathrm{til}} \cdot s = -k_{\mathrm{til}} \cdot \frac{\partial h}{\partial x} \quad (3)$$

Where: k_{til} is the tillage transport coefficient (kg m^{-1} yr^{-1}), *s* is the local slope (%), *h* is the height at a given point of the hillslope (m), and *x* is the distance in horizontal direction (m) (Govers et al., 1994). The local tillage-induced erosion or deposition rate E_{til} (kg m^{-2} yr^{-1}) has been calculated as

$$E_{\mathrm{til}} = -\frac{\partial Q_{\mathrm{til}}}{\partial x} = k_{\mathrm{til}} \cdot \frac{\partial^2 h}{\partial x^2} \quad (4)$$

As tillage erosion is governed by the change in slope gradient and not by the slope gradient itself, erosion mainly takes place on convexities and soil accumulates in concavities (Govers et al., 1994; Van Oost, Govers, & Desmet, 2000). Moreover, erosion and deposition in the region are governed by the edge of kettle holes and, to a lesser extent, field borders (Wilken et al., 2017).

The tillage transport coefficient k_{til} depends on the tillage implement, tillage speed, tillage depths, bulk density, texture, and soil moisture at time of tillage (Van Oost, Govers, et al., 2006). For our study, we used a constant k_{til} value of 350 kg m^{-1} yr^{-1}, which was recently determined for this region (Wilken, Ketterer, Koszinski, Sommer, & Fiener, 2020). As k_{til} only determines the intensity of the calculated erosion rates, the parameterization of k_{til} is not sensitive to the spatial pattern of tillage translocation. Hence, the absolute erosion rates do not influence the results of the EVI correlation analysis carried out in this study.

The water erosion pattern was calculated according to a slightly modified approach of the revised usoil loss equation (RUSLE; Renard, Foster, Weesies, McCool, & Yoder, 1997) described in detail in Van Oost et al. (2000). Erosion, sediment transport, and deposition are based on the local transport capacity T_c (kg m^{-1} yr^{-1}), which multiplies the RUSLE factors *R*, *C*, *K*, *P* (see Renard et al., 1997), and LS_{2D} (Desmet & Govers (1996) with a transport capacity coefficient (k_{tc}; m) (Equation 5).

$$T_c = k_{\mathrm{tc}} \cdot R \cdot C \cdot K \cdot LS_{2D} \cdot P \quad (5)$$

The parameterization of the water erosion module follows Wilken et al. (2020) with a k_{tc} value of 150 m, *R* factor of 450 MJ mm ha^{-1} hr^{-1} yr^{-1}, *K* factor of 0.027 Mg ha hr ha^{-1} MJ^{-1} mm^{-1}, and *P* factor of 1.0 (i.e., no erosion control practices). The *C* factor

was calculated for a conventional small grain tillage crop rotation that is typical for the study region (winter rapeseed—winter wheat—winter barley, cultivated without cover crops; Wilken et al., 2018). Maize was not considered as it is only relevant in recent crop rotations (Gömann & Kreins, 2012; Vogel, Deumlich, & Kaupenjohann, 2016). Following the procedure of Schwertmann, Vogl, and Kainz (1987), this crop rotation resulted in a *C* factor of 0.081. The LS_{2D} is a grid cell–specific topographic factor calculated following Desmet and Govers (1996) using the digital elevation model (DEM; derived from airborne laserscanning; original spatial resolution of 1 m resampled to 5 m) (Landesamt für Umwelt & Landesvermessung und Geobasisinformation Brandenburg, 2012).

As most topsoil layers (Ap-horizons) of the study area show a sandy-loam soil texture (e.g., Deumlich et al., 2017), wind erosion is of minor importance (Deumlich, Funk, Frielinghaus, Schmidt, & Nitzsche, 2006). Hence, the spatial pattern of total erosion results from adding up tillage and water erosion per grid cell. In the following, the modeled tillage, water, and total erosion pattern based on SPEROS-C will be referred to as E_{til}, E_{wat}, and E_{tot} respectively. To avoid misinterpretations due to mixed pixels along field borders, a 30 m buffer inside each field border was excluded from the analysis. For the same reason, a 15 m buffer around the kettle holes was removed from the data. Note that using buffers at field borders and around kettle holes also means that areas of potentially strong tillage erosion and deposition are excluded. Extremely high erosion or deposition rates of single grid cells often resulting from DEM artefacts or errors in land use classification were also excluded to reduce skewness and meet the requirements for regression analysis (erosion >35 and <−35 Mg ha^{-1}; ca. 0.01% of the data).

2.4 | Statistical analysis

Three approaches were performed to analyze the potential effect of soil redistribution on crop biomass: (a) The EVI was related to E_{til}, E_{wat}, and E_{tot} on a pixel-by-pixel basis for a single field (no. of pixels $n = 9{,}290$). (b) The standardized EVI (EVI_z) was related to E_{tot} for all fields with the same crop on a pixel-by-pixel basis (no. of pixels: barley $n \approx 60{,}000$, maize $n \approx 150{,}000$, winter rapeseed $n \approx 220{,}000$, winter wheat $n \approx 800{,}000$). The standardization was applied to focus on in-field variability and reduce between-field variabilty. (c) To reduce small-scale scattering of the EVI and EVI_z caused by other influences than soil redistribution, all crop-specific EVI and EVI_z values were grouped into classes of E_{tot} and E_{til} (size of each class: 5 Mg ha^{-1} yr^{-1}). Subsequently, mean EVI values were calculated per E_{tot} and E_{til} class.

The strength of the interrelation between EVI and E_{til}, E_{wat}, or E_{tot} was calculated using linear and nonlinear regression analysis (polynomials degree = 1 or 2) and quantified by the adjusted coefficient of determination (R^2). The wet and normal year were analyzed separately to identify potential effects of seasonal differences in rainfall on EVI and EVI_z patterns. Moreover, all analyses were performed for each crop separately. To determine whether two coefficients of determination (and hence slope) differed significantly, we used the test according to Hotelling (1931, 1940) in the case of overlapping pairs of variables (i.e., for the example field data) or according to Fisher (1921) in the case of independent samples (i.e., for the landscape-scale data).

To quantify the net effect of soil redistribution (E_{tot}) on the EVI as proxy for biomass production on landscape scale, the differences of EVI at sites of little erosion (−5 to 5 Mg ha^{-1} yr^{-1}) taken as baseline and the EVI of all other sites were calculated and averaged per crop. The significance of the net effect was determined using Student's *t* test or alternatively Wilcoxon rank sum-test when the samples were not normally distributed. All statistical analyses were performed using R version 3.6.1 (R Core Team, 2019).

3 | RESULTS

Analyzing an exemplary field (35 ha) cropped with winter wheat in both years illustrated the similarity between patterns of E_{tot} and EVI as a proxy for biomass (Figure 4). The lowest EVI values were found on hill shoulders and top slopes where most E_{til} and E_{tot} occurred, while the highest EVI values were found in the depositional areas (positive E_{til} and E_{tot} and partly positive E_{wat}). No obvious similarity in pattern between E_{wat} and EVI can be found, partly because E_{wat} is substantially smaller than E_{til}.

Taking a closer look at the general behavior of the relation between EVI and E_{til}, E_{wat}, or E_{tot} for the exemplary wheat field revealed that a pixel-by-pixel comparison resulted in a highly significant linear regression between EVI and E_{til} or E_{tot} in both years ($R^2 = 0.15…0.19$, p *value* < .001; Figure 5a,b). This indicated that 15–19% of the total variation was due to soil redistribution, while the many other reasons for differences in EVI including error contributed 81–85%. The coefficients of determination for E_{wat}, although very highly significant, are not given in Figure 5 due to the statistically unfavorable, highly skewed distribution of data that mainly resulted from former kettle holes that still caused depressions capturing large amount of sediments. However, the combination of E_{wat} and E_{til} in E_{tot}, which did not have this problem, always had a higher R^2 than E_{til} alone. The difference, although small due to the much smaller E_{wat} than E_{til} rates, was even very highly significant in the wet year according to the Hotelling test. The patterns of E_{wat} and E_{til} were almost completely independent ($R^2 = .008$) and thus contributed both independently to the EVI patterns. In the normal year, EVI showed much more variability due to soil redistribution compared to the wet year, and the relations to E_{til} and E_{tot} were highly significantly steeper and closer (p value < .001).

Reducing the effects of other causes of EVI variability to extract the influence of E_{tot} by calculating mean values per soil redistribution classes (Figure 5d,e) revealed that in the wet year, a reduction in the EVI mainly occurred at losses above 10 Mg ha^{-1} yr^{-1}, while in the normal year, any increase in erosion rate caused a decrease in EVI. In depositional areas, EVI only increased up to a deposition rate of 10 Mg ha^{-1} yr^{-1}, while higher rates did not increase EVI anymore. The increase in EVI explained by soil redistribution was small in the

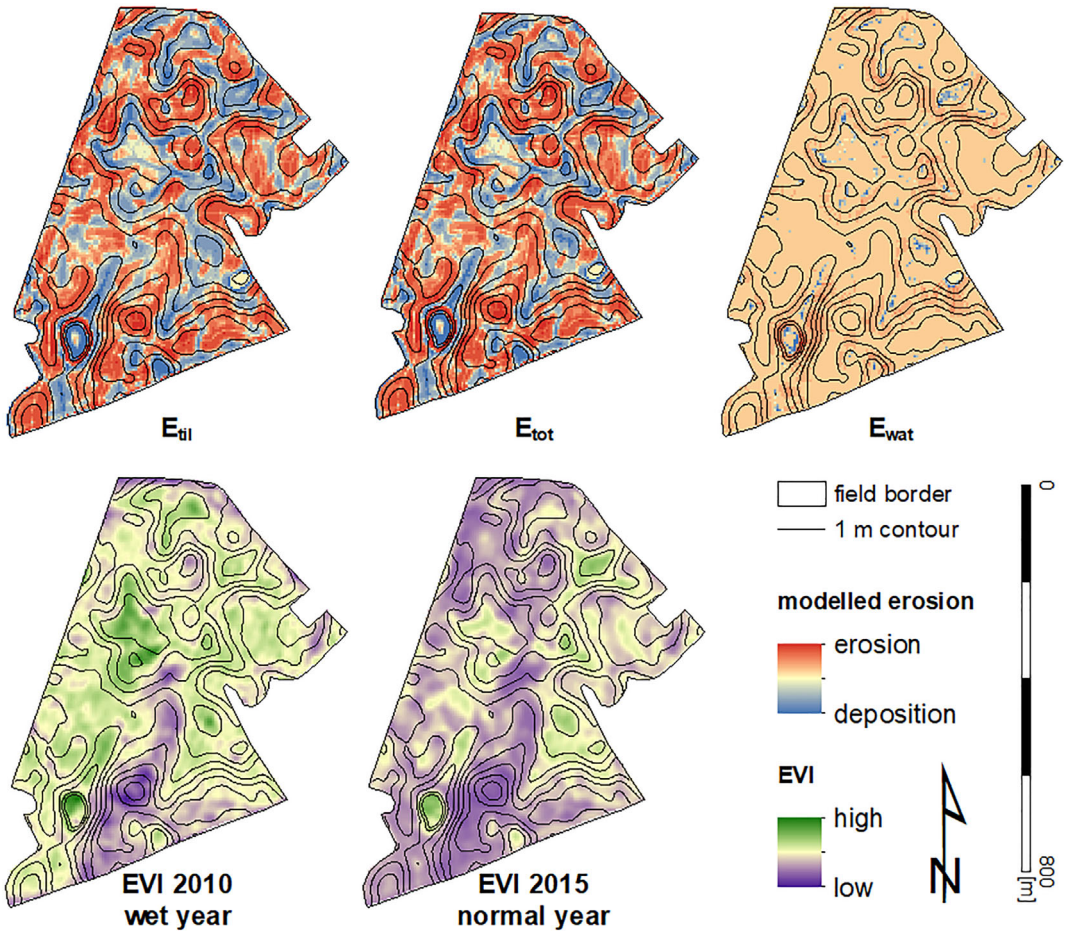

FIGURE 4 Spatial patterns of modeled tillage erosion (E_{til}), total erosion (E_{tot}), and water erosion (E_{wat}) and enhanced vegetation index (EVI) for the wet year 2010 and the normal year 2015 with contour lines of 1 m derived from the digital elevation model (DEM). Results are shown for an exemplary winter wheat field (35 ha, 53.36°N, 13.66°E) [Colour figure can be viewed at wileyonlinelibrary.com]

wet year (difference between the minimum and the flattening was about 0.13 for E_{til} and 0.15 for E_{tot}), while in the normal year, it was substantial (about 0.22 for E_{til} and 0.26 for E_{tot}). Remarkably, the within-field variation of EVI caused by soil redistribution was larger in the normal year than the difference between the wet and the normal year on sites with the lowest soil redistribution rates (0.15 for E_{til} and E_{tot}).

The general behavior of the relation between the EVI and E_{tot} as well as E_{til} did not only hold true for the exemplary winter wheat field (Figures 4 and 5) but was also found when the standardized EVI (EVI_z) of all fields of the entire study area was considered for the different crop types and years (Figure 6). As the standardization removes differences between fields, EVI_z describes the in-field variability of the EVI. Based on the pixel-by-pixel comparison (Figure 6a–d), the relation between E_{tot} and EVI_z could be fairly well described with first- or second-order polynomials. The winter rapeseed EVI_z had the strongest relation to E_{tot} ($R^2 = .16$ and .30 in the wet and normal year, respectively), that is, erosion explained 16% or even 30% of the total variation that occurred within many ordinarily farmed fields belonging to different farmers with multiple reasons for variation. The strength of the relation decreased in the order winter wheat, maize, and winter barley. This order was true in the wet and in the normal year, but for winter barley, the effect became very small in the wet year.

Regarding the classified data (Figure 6e–h), the functional relation was sigmoid for winter rapeseed and maize, indicating that very high erosion or deposition rates only caused small additional effects compared to lower rates. For winter wheat, the effect appeared to increase linearly over the entire range. In contrast to the example field shown in Figure 5, both years were not separated by a shift, which was an effect of normalizing the data. Nevertheless, the EVI_z at the erosional sites was significantly lower in the normal than in the wet year for all crops.

The net effect on the landscape scale that results from EVI gains on depositional sites and EVI losses on eroded sites was greatest for maize (based on no. of pixels $n \approx 150{,}000$) with a reduction of −10.2% in the wet and −8.5% in the normal year compared to areas with more or less no erosion and deposition (Figure 7). In the wet year, there was nearly no change of the EVI related to E_{tot} for winter wheat (−1.4%; $n \approx 800{,}000$) and winter rapeseed (−0.6%; $n \approx 220{,}000$). In these cases, higher EVI values at depositional sites outweighed lower EVI values at erosional sites. However, in the

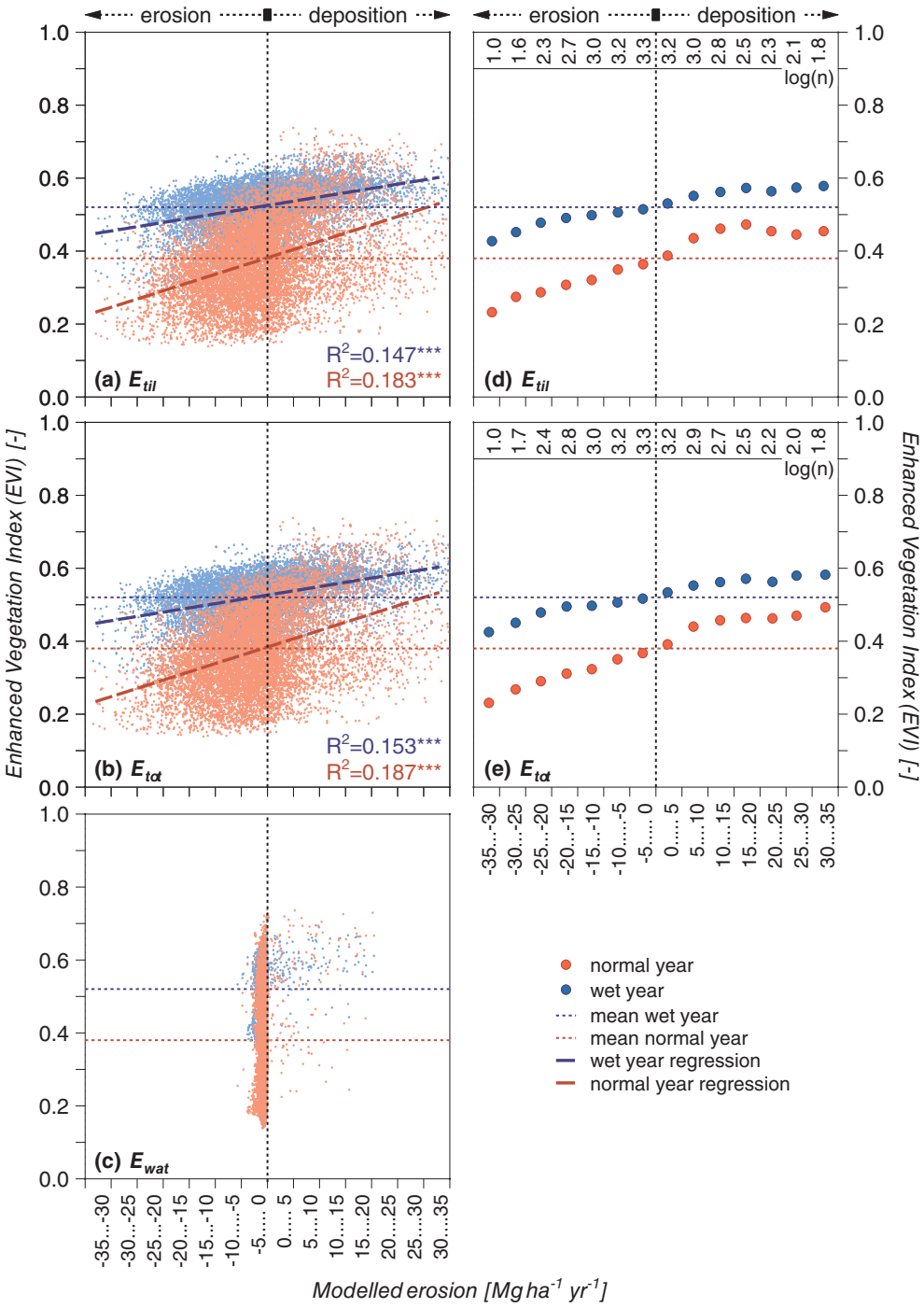

FIGURE 5 Enhanced vegetation index (EVI) versus modeled tillage erosion (E_{til}, a), total erosion (E_{tot}, b), and water erosion (E_{wat}, c) for a single exemplary winter wheat field (also shown in Figure 4) in the wet (blue) and normal year (red). The horizontal lines denote the mean EVI in the wet (blue line) and normal year (red line). Left: pixel-by-pixel comparison (no. of pixels n = 9,290) with dashed lines showing linear regression models. Stars denote the significance level of the adjusted coefficient of determination R^2 (*p value < .05, **p value < .01, ***p value < .001). Right: comparison of mean EVI for 5 Mg ha^{-1} a^{-1} E_{til} (d) and E_{tot} classes (e). The number of values per class is given by the common logarithm of the respective number [Colour figure can be viewed at wileyonlinelibrary.com]

normal year, significant reductions due to E_{tot} were observed for winter rapeseed (−4.5%) and winter wheat (−6.4%). Interestingly, there was a significant increase in the winter barley EVI in the wet year (+3.7%; $n \approx$ 60,000), but no significant influence of E_{tot} in the normal year (+0.2%).

4 | DISCUSSION

The impact of soil erosion on crop biomass has already been investigated in a large number of studies on field-scale, which is exemplarily shown for more or less standardized desurfacing experiments (Figure 1). Although the results vary greatly, a clear decline in yields due to erosion can be seen. In comparison to desurfacing studies, our approach considered real soil redistribution that also included soil deposition on the large scale in the hummocky ground moraine landscape of Northeast Germany. Here, soil redistribution was found to be dominated by tillage erosion that led to in-field variation of the EVI and, hence, biomass patterns. All crops had a lower EVI on eroded sites. Taking depositional sites into account as well, a net reduction effect due to soil redistribution was confirmed for three out of four crop types (Figure 7).

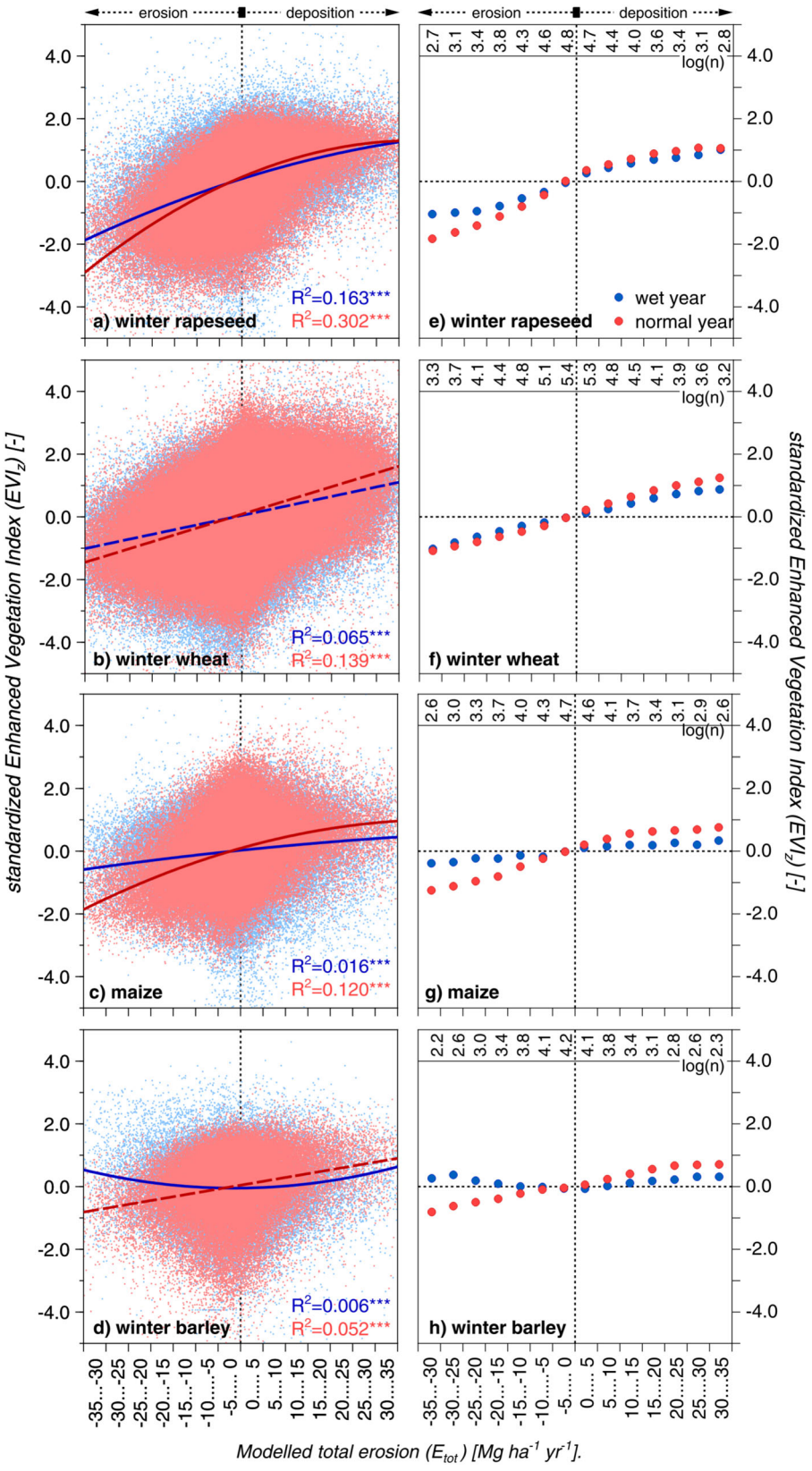

FIGURE 6 Standardized enhanced vegetation index (EVI_z) versus modelled total erosion (E_{tot}) for the four crop types winter rapeseed (a, $n \approx 220{,}000$), winter wheat (b, $n \approx 800{,}000$), maize (c, $n \approx 150{,}000$), and winter barley (d, $n \approx 60{,}000$) in the wet (blue) and normal year (red) for the entire study area. Left: pixel-by-pixel comparison with regression lines shown for first-(dashed lines) and second-degree polynomial models (solid lines). Stars denote the significance level of the adjusted coefficient of determination R^2 (*p value < .05, **p value < .01, ***p value < .001). Right: comparison of mean EVI_z for 5 Mg ha^{-1} yr^{-1} E_{tot} classes ([e] winter rapeseed, [f] winter wheat, [g] maize, [h] winter barley). The number of values per class is given by the common logarithm of the respective number [Colour figure can be viewed at wileyonlinelibrary.com]

4.1 | Methodological considerations

The regressions between EVI or EVI_z and E_{tot} on a pixel-by-pixel basis were highly significant but had, in some cases, little explanatory power (wet year in Figure 6b–d). This was not surprising because due to the relatively high spatial resolution of the EVI and the calculated total erosion, many effects influencing crop growth contribute to the total variation. The EVI contained existing small-scale differences in

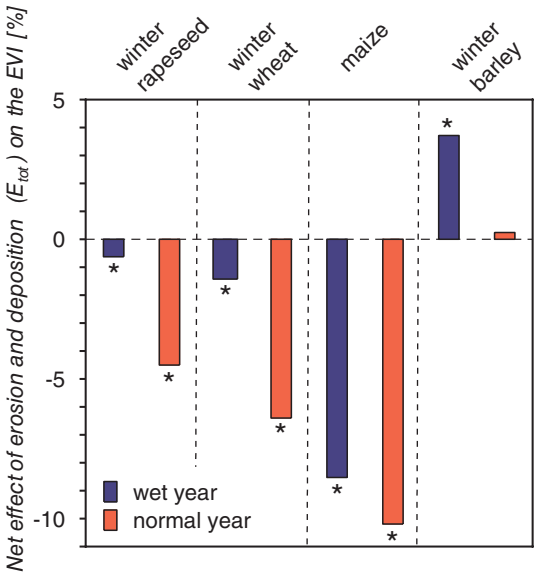

FIGURE 7 Net effect of soil redistribution (modeled total erosion E_{tot}) on the enhanced vegetation index (EVI) of the four crop types winter rapeseed, winter wheat, maize, and winter barley in the wet and normal year. Stars denote the significance (p value < .001) of the net effect of soil redistribution (zero line; class −5 to 5 Mg ha^{-1} yr^{-1}). Areas affected by soil redistribution vary among crops (45% for winter wheat, 41% for maize, 50% for winter rapeseed, and 54% for winter barley) [Colour figure can be viewed at wileyonlinelibrary.com]

biomass, for example, due to tractor lanes or local differences in management (e.g., fertilization, varieties, pests, management mistakes) and is also sensitive to local environmental differences (e.g., windbreak, shadows, exposition). Other factors causing uneven crop growth are for example short-range (<1 km) variation in rainfall (Fiener & Auerswald, 2009) and wind erosion. Although wind erosion is relevant for sandy topsoils across Germany, it is more or less negligible for our study area (Deumlich et al., 2006; Sommer et al., 2008). Besides these reasons of true variability, the pixel-by-pixel comparison of different high-resolution products is always confronted with some errors in geo-referencing, which inevitably result in an (unevenly distributed) offset of one or two pixels between the EVI and the DEM. Despite the manifold reasons for growth variability on fields managed by many farmers, it was remarkable that still up to 30% of the total variability was explained by soil redistribution. This interpretation of a strong erosion effect deteriorating the water capacity of the soils is corroborated by the fact that, in wet years, the influence of erosion decreased.

We can safely assume that most of the erosion-related pattern of EVI was not caused by recent erosion (e.g., due to water losses by runoff) but related to long-term soil truncation and colluviation, which modify important soil properties influencing plant growth and crop biomass (e.g., rooting depth, bulk density, water and nutrient availability, etc.). Nevertheless, the modeled erosion patterns served well as proxy variables for long-term soil truncation or colluviation even though they were based on recent data of soil use valid for the last 60 years (Wilken et al., 2020). Most changes in erosion parameters like rain erosivity, cropping sequence, or tillage intensity, which might have happened, would not change the soil redistribution pattern but only the absolute amount. Thus, they cannot influence our analysis based on the patterns except for two exceptions: First, the relative contribution of water and tillage erosion may change with different parameter values. This influence can be regarded small, given the large absolute difference between both erosion types under recent management. Moreover, increasing tillage intensity also decreases soil cover and thus increases tillage and water erosion simultaneously. Second, the large fields that can be found nowadays were set into practice during the socialistic era and are only about 60 years old (Bayerl, 2006). Before, many more field borders existed, which particularly govern tillage erosion. The influence of historic field borders, as far as it still exists after 60 years, will contribute to the scatter at pixel resolution, while it is eliminated in the classified analysis.

Another pitfall of our proxies would be to neglect other processes that influence EVI and create a similar pattern like E_{til} and E_{wat} and, thus, would erroneously be attributed to soil redistribution. There are mainly two processes that produce similar patterns. One is solifluction during the Pleistocene, which creates a similar pattern as E_{til}, because its driving principle is identical to that of tillage erosion: during frost, the soil is lifted parallel to the soil surface, but during thawing, it settles back vertically causing a net movement downslope. However, areal soil observations (e.g., Figure 3) indicate strong soil translocation and profile truncation, which must have happened after soil genesis and cannot be of Pleistocene origin. The other potential process creating a similar pattern is surface runoff (plus runon infiltration) or interflow, which causes water deficit in upslope positions and a longer and better water supply in downslope positions. However, lateral water flow should be larger in wet years, while we observed consistently more pronounced patterns in the normal year. An often-used argument is that the potential effect of erosion on crop biomass or yields is just resulting from the coincidence of water erosion and soil moisture patterns modified by lateral fluxes (Heckrath et al., 2005; Moulin, Anderson, & Mellinger, 1994; Stone et al., 1985), which has a particular effect in dry years. This does not hold true within this study, as the low precipitation of only 211 mm during the vegetation period in the normal year is not sufficient to cause substantial lateral water flux.

Overall, our findings of tillage erosion being the dominant erosion process in the region are also confirmed by other local studies conducted in the young moraine landscape of Northeast Germany. The dramatic increase of sedimentation rates in kettle holes and at footslopes, which was dated on the second half of the 20th century, was related to increasing mechanization of tillage practices (Frielinghaus & Vahrson, 1998; Keller, Sandin, Colombi, Horn, & Or, 2019; Li et al., 2002; Van der Meij et al., 2019). Wilken et al. (2020) assessed soil redistribution by tillage and water in a small, representative sub-catchment (ca. 4.2 ha) in the centre of our study area using $^{239+240}$Pu and an inverse modeling analysis. The results showed that soil erosion by water is an order of magnitude lower compared to tillage erosion (Wilken et al., 2020) and, thus, support our findings that tillage erosion and the corresponding patterns in soil properties and plant growth conditions are dominant in this region.

It is important to note that in our study, EVI is only a proxy for crop biomass. However, EVI was already related to crop biomass in other studies. For example, a strong relationship between EVI and fresh biomass of lucerne (*Medicago sativa* L.) was found at a test site in our study area (Wehrhan et al., 2016) and between EVI and winter wheat biomass in China (Jin et al., 2015, 2017). Jin et al. (2015) found an exponential relation of EVI and biomass. Application of this relation to convert our winter wheat EVI (range from 0.2 to 0.7) into biomass would result in a more pronounced effect of total erosion on biomass compared to the effect on the EVI. Although a direct comparison of Jin et al. (2015) with this study is difficult, it indicates that the relative reduction of the EVI due to soil redistribution is a conservative estimate of the potentially higher reduction of crop biomass.

4.2 | Response of EVI to soil erosion patterns

In general, our analysis of the EVI and EVI_z revealed that erosion-induced truncation and accumulation had a larger influence on crop biomass in a normal year compared to a wet year. This might be traced back to water limitation due to lower water holding capacity of truncated soil profiles and improvements on colluvial soils. The sigmoidal behaviour at the lower end (high soil losses), which comprised about 2% of our data, suggests that at this end, most of the soil has already been lost and crops already utilize the unweathered moraine sediments. Once the complete soil is lost, no further decrease in crop growth will occur as long as moraine sediments are still available. The flattening at the upper end (high accumulation rates), which again comprised about 2% of our data, may indicate that the colluvial material already exceeds effective rooting depth of the crops and an increase did not have further positive effects. The almost linear response function of winter wheat may be caused by an especially large rooting depth (Araki & Iijima, 2001; Fan, McConkey, Wang, & Janzen, 2016; Thorup-Kristensen, Salmerón Cortasa, & Loges, 2009). However, the interpretation of the response functions varying between the crops is difficult because we analyzed only one wet and one normal year. Within the denominations wet and normal, precipitation between months may vary considerably. Given that the temporal course of ontogenesis differs between crops, the specific rain distribution in 2010 or 2015 may have been more favourable for one crop than for the other. The fact that the response of winter rapeseed was strong in the normal and in the wet year, while the response of winter barley was small in both years, suggests that at least some of the differences are crop specific and not due to the specific distribution of precipitation in both years. It is also interesting to note that although winter rapeseed shows the highest in-field variation, maize seems to be the crop type most affected on landscape scale. This might be traced back to the already mentioned differences (e.g., regional precipitation patterns, management, etc.) leading to fields with generally low or high biomass. The underlying reasons for the different behaviour of the crop types are beyond the scope of this study and would require different data and an approach related to yield physiology.

Overall, our analysis showed highly significant relations between soil redistribution and EVI/biomass patterns in a hummocky ground moraine landscape. Similar results were found in the hummocky moraine landscape of Denmark (Heckrath et al., 2005), in the morainic area of Minnesota, North America (Papiernik et al., 2005) or in the young moraine landscape of Ontario, Canada (Battiston et al., 1987). Compared to Battiston et al. (1987) who quantified the yield decline at eroded areas to be −3.6%, we even found a net effect including the EVI gains on depositional sites to be −10.2% in the wet and −8.5% in the normal year for maize. In addition to the net effect, redistribution induces a pronounced heterogeneity that brings about management problems like uneven fertilizer demand or uneven ripening.

Soil redistribution was dominated by tillage, but the effect of water erosion was still detectable. This relation was tighter and steeper in the normal year. In the context of climate change, potentially introducing more dry spells in spring and early summer (Gerstengarbe et al., 2003; Heinrich et al., 2018), the negative effect of soil redistribution on crop biomass might become even more important, especially for winter wheat as the dominant crop type in the studied region. This also holds true for maize, which seems to be the crop type mostly affected by soil redistribution (Figure 7). This is particularly critical, as maize has become an important energy crop that is increasingly cultivated (Hoffmann et al., 2018; Peichl, Thober, Meyer, & Samaniego, 2018; Vogel et al., 2016). In this respect, it is also important to note that these hummocky landscapes, which are highly prone to tillage erosion, cover an area of approximately 1.8×10^6 km^2 globally (comparable to the size of Libya or five-times the size of Germany), whereby half of it is or was used as arable land (Sommer, Fiedler, Glatzel, & Kleber, 2004).

5 | CONCLUSIONS

Soil redistribution feedbacks on above ground crop biomass of different crop types were investigated by the comparison of the EVI as a proxy for crop biomass with modeled tillage, water, and total erosion patterns in the hummocky ground moraine landscape of Northeast Germany. The differences in the EVI between erosional and depositional sites were more pronounced in the analyzed normal year compared to the wet year. On average, total erosion patterns explained 6% of the within-field variation of EVI_z in a wet and 15% in a normal year. It was shown that the erosion-related variation can be much higher for individual fields and for specific crops. Although soil redistribution can lead to beneficial soil properties at depositional areas and hence, to higher EVI/biomass, the net effect of erosion and deposition on the EVI resulted in an average change of −5% for a normal year. As water erosion only contributed little to the patterns of total soil redistribution in this landscape, tillage erosion was found to be the dominant soil redistribution process in this region. This stresses an urgent need to consider tillage as major soil redistribution process affecting crop biomass production.

ACKNOWLEDGMENT

This work was supported by ZALF's research station at Dedelow (G. Verch et al.) and financed by the DFG project "TilEro" (FI-1216/12-1, SO-302/12-1).

CONFLICT OF INTEREST

The authors declare that there is no conflict of interest that could be perceived as prejudicing the impartiality of the research reported.

DATA AVAILABILITY STATEMENT

The data that support the findings of this study are available from the corresponding author upon reasonable request.

ORCID

Peter Fiener https://orcid.org/0000-0001-6244-4705

REFERENCES

Allen, B. L., Cochran, V. L., Ceasar, T., & Tanaka, D. L. (2011). Long-term effects of topsoil removal on soil productivity factors, wheat yield and protein content. *Archives of Agronomy and Soil Science*, *57*(3), 293–303. https://doi.org/10.1080/03650340903302294.

Amundson, R., Berhe, A. A., Hopmans, J. W., Olson, C., Sztein, A. E., & Sparks, D. L. (2015). Soil and human security in the 21st century. *Science*, *348*, 1261071. https://doi.org/10.1126/science.1261071

Anderson, G. (1998). Genesis of hummocky moraine in the Bolmen area, southwestern Sweden. *Boreas*, *27*, 55–67. https://doi.org/10.1111/j.1502-3885.1998.tb00867.x

Araki, H., & Iijima, M. (2001). Deep rooting in winter wheat: Rooting nodes of deep roots in two cultivars with deep and shallow root systems. *Plant Production Science*, *4*(3), 215–219. https://doi.org/10.1626/pps.4.215

Bakker, M. M., Govers, G., & Rounsevell, M. D. A. (2004). The crop productivity–erosion relationship: An analysis based on experimental work. *Catena*, *57*(1), 55–76. https://doi.org/10.1016/j.catena.2003.07.002

Battiston, L. A., Miller, M. H., & Shelton, I. J. (1987). Soil erosion and corn yield in Ontario. I. Field Evaluation. *Canadian Journal of Soil Science*, *67*, 731–745. https://doi.org/10.4141/cjss87-072

Bayerl, G. (2006). Geschichte der Landnutzung in der Region Barnim-Uckermark. In *Materialien der Interdisziplinären Arbeitsgruppe Zukunftsorientierte Nutzung ländlicher Räume-LandInnovation, Nr* (Vol. 12). Berlin: Germany.

Chander, G., Haque, M. O., Sampath, A., Brunn, A., Trosset, G., Hoffmann, D., … Anderson, C. (2013). Radiometric and geometric assessment of data from the RapidEye constellation of satellites. *International Journal of Remote Sensing*, *34*(16), 5905–5925. https://doi.org/10.1080/01431161.2013.798877

Chi, B.-L., Bing, C.-S., Walley, F., & Yates, T. (2009). Topographic indices and yield variability in a rolling landscape of western Canada. *Pedosphere*, *19*(3), 362–370. https://doi.org/10.1016/S1002-0160(09)60127-2

Chirinda, N., Roncossek, S. D., Heckrath, G., Elsgaard, L., Thomsen, I. K., & Olesen, J. E. (2014). Root and soil carbon distribution at shoulderslope and footslope positions of temperate toposequences cropped to winter wheat. *Catena*, *123*, 99–105. https://doi.org/10.1016/j.catena.2014.07.012

Cooley, T., Anderson, G. P., Felde, G. W., Hoke, M. L., Ratkowski, A. J., Chetwynd, J. H., … Lewis, P. (2002). *FLAASH, a MODTRAN4-based atmospheric correction algorithm, its application and validation*. Paper presented at the IEEE international geoscience and remote sensing symposium, Toronto, Ontario, Canada.

R Core Team. (2019). *A language and environment for statistical computing*. Vienna, Austria: R Foundation for Statistical Computing.

De Alba, S., Lindstrom, M., Schumacher, T. E., & Malo, D. D. (2004). Soil landscape evolution due to soil redistribution by tillage: A new conceptual model of soil catena evolution in agricultural landscapes. *Catena*, *58*(1), 77–100. https://doi.org/10.1016/j.catena.2003.12.004

Den Biggelaar, C., Lal, R., Wiebe, K., & Breneman, V. (2001). The impact of soil erosion on crop yields in North America. In D. L. Sparks (Ed.), *Advances in agronomy* (Vol. 72, pp. 1–52). Boston, MA: Academic Press.

Den Biggelaar, C., Lal, R., Wiebe, K., & Breneman, V. (2003). The global impact of soil erosion on productivity I: Absolute and relative erosion-induced yield losses. In *Advances in agronomy* (Vol. 81, pp. 1–48). Boston, MA: Academic Press.

Desmet, P. J. J., & Govers, G. (1996). A GIS procedure for automatically calculating the USLE LS factor on topographically complex landscape units. *Journal of Soil and Water Conservation*, *51*(5), 427–433.

Deumlich, D., Funk, R., Frielinghaus, M., Schmidt, W.-A., & Nitzsche, O. (2006). Basics of effective erosion control in German agriculture. *Journal of Plant Nutrition and Soil Science*, *169*(3), 370–381. https://doi.org/10.1002/jpln.200621983

Deumlich, D., Rogasik, H., Hierold, W., Onasch, I., Völker, L., & Sommer, M. (2017). The CarboZALF-D manipulation experiment–experimental design and SOC patterns. *International Journal of Environmental & Agriculture Research*, *3*(1), 40–50.

Deumlich, D., Schmidt, R., & Sommer, M. (2010). A multiscale soil-landform relationship in the glacial-drift area based on digital terrain analysis and soil attributes. *Journal of Plant Nutrition and Soil Science*, *173*(6), 843–851. https://doi.org/10.1002/jpln.200900094

DWD Climate Data Center (CDC). (2018a). *Historical hourly station observations of 2m air temperature and humidity for Germany, version v006*.

DWD Climate Data Center (CDC). (2018b). *Historical Hourly Station Observations of Precipitation for Germany, Version v006*.

ERDAS Inc. (2008). *Erdas Field Guide*. Atlanta, GA: ERDAS Inc.

ESRI. (2017). *ArcMap Desktop version 10.5.1*. Redlands, CA: Environmental Systems Research Institute.

Fan, J., McConkey, B. G., Wang, H., & Janzen, H. H. (2016). Root distribution by depth for temperate agricultural crops. *Field Crops Research*, *189*, 68–74. https://doi.org/10.1016/j.fcr.2016.02.013

Fiener, P., & Auerswald, K. (2009). Spatial variability of rainfall on a sub-kilometre scale. *Earth Surface Processes and Landforms*, *34*(6), 848–859. https://doi.org/10.1002/esp.1779

Fiener, P., Wilken, F., Aldana-Jague, E., Deumlich, D., Gómez, J. A., Guzmán, G., … Wexler, R. (2018). Uncertainties in assessing tillage erosion – How appropriate are our measuring techniques? *Geomorphology*, *304*, 214–225. https://doi.org/10.1016/j.geomorph.2017.12.031

Fisher, R. A. (1921). On the "probable error" of a coefficient of correlation deduced from a small sample. *Metron*, *1*, 3–32.

Frielinghaus, M., & Vahrson, W.-G. (1998). Soil translocation by water erosion from agricultural cropland into wet depressions (morainic kettle holes). *Soil and Tillage Research*, *46*, 23–30. https://doi.org/10.1016/S0167-1987(98)80104-9

Gao, X., Huete, A. R., Ni, W., & Miura, T. (2000). Optical-biophysical relationships of vegetation spectra without background contamination. *Remote Sensing of Environment*, *74*, 609–620. https://doi.org/10.1016/S0034-4257(00)00150-4

Gerke, H. H., & Hierold, W. (2012). Vertical bulk density distribution in C-horizons from marley till as indicator for erosion history in a hummocky post-glacial soil landscape. *Soil and Tillage Research*, *125*, 116–122. https://doi.org/10.1016/j.still.2012.06.005

Gerke, H. H., Rieckh, H., & Sommer, M. (2016). Interactions between crop, water, and dissolved organic and inorganic carbon in a hummocky landscape with erosion-affected pedogenesis. *Soil and Tillage Research*, *156*, 230–244. https://doi.org/10.1016/j.still.2015.09.003

Gerstengarbe, F.-W., Badeck, F., Hattermann, F., Krysanova, V., Lahmer, W., Lasch, P., … Werner, P. C. (2003). *Studie zur klimatischen Entwicklung im Land Brandenburg bis 2055 und deren Auswirkungen auf den Wasserhaushalt, die Forst- und Landwirtschaft sowie die Ableitung erster Perspektiven*. PIK Report, (83). Potsdam Institute for Climate Impact Research (PIK), Potsdam.

Gömann, H., & Kreins, P. (2012). Landnutzungsänderungen in Deutschlands landwirtschaft. Rückläufige anbaudiversität hat viele ursachen. *Mais*, *39*(3), 118–122.

Gorji, M., Rafahi, H., & Shahoee, S. (2008). Effects of surface soil removal (simulated erosion) and fertilizer application on wheat yield. *Journal of Agricultural Science and Technology*, *10*(4), 317–323.

Govers, G., Lobb, D. A., & Quine, T. A. (1999). Preface-tillage erosion and translocation: Emergence of a new paradigm in soil erosion research. *Soil & Tillage Research*, *51*(3–4), 167–174. https://doi.org/10.1016/S0167-1987(99)00035-5

Govers, G., Poesen, J., & Goossens, D. (2004). Soil erosion-processes, damages and countermeasures. In P. Schjønning, S. Elmholt, & B. T. Christensen (Eds.), *Managing soil quality-challenges in modern agriculture* (pp. 199–217). Oxford, UK: CABI Publishing.

Govers, G., Quine, T. A., Desmet, P. J. J., & Walling, D. E. (1996). The relative contribution of soil tillage and overland flow erosion to soil redistribution on agricultural land. *Earth Surface Processes and Landforms*, *21*, 929–946. https://doi.org/10.1002/(SICI)1096-9837(199610)21:10<929::AID-ESP631>3.0.CO;2-C

Govers, G., Vandaele, K., Desmet, P., Poesen, J., & Bunte, K. (1994). The role of tillage in soil redistribution on hillslopes. *European Journal of Soil Science*, *45*(4), 469–478. https://doi.org/10.1111/j.1365-2389.1994.tb00532.x

Heckrath, G., Djurhuus, J., Quine, T. A., Van Oost, K., Govers, G., & Zhang, Y. (2005). Tillage erosion and its effect on soil properties and crop yield in Denmark. *Journal of Environmental Quality*, *34*(1), 312–324. https://doi.org/10.2134/jeq2005.0312a.

Heinrich, I., Balanzategui, D., Bens, O., Blasch, G., Blume, T., Böttcher, F., … Wilken, F. (2018). Interdisciplinary geo-ecological research across time scales in the northeast German lowland observatory (TERENO-NE). *Vadose Zone Journal*, *17*(180116), 1–25. https://doi.org/10.2136/vzj2018.06.0116

Herbrich, M., Gerke, H. H., & Sommer, M. (2018). Root development of winter wheat in erosion-affected soils depending on the position in a hummocky ground moraine soil landscape. *Journal of Plant Nutrition and Soil Science*, *181*(2), 147–157. https://doi.org/10.1002/jpln.201600536

Hoffmann, M., Pohl, M., Jurisch, N., Prescher, A. K., Mendez Campa, E., Hagemann, U., … Augustin, J. (2018). Maize carbon dynamics are driven by soil erosion state and plant phenology rather than nitrogen fertilization form. *Soil and Tillage Research*, *175*, 255–266. https://doi.org/10.1016/j.still.2017.09.004

Hotelling, H. (1931). The generalization of Student's ratio. *The Annals of Mathematical Statistics*, *2*(3), 360–378.

Hotelling, H. (1940). The teaching of statistics. *The Annals of Mathematical Statistics*, *11*(4), 457–470.

Huete, A., Didan, K., Miura, T., Rodriguez, E. P., Gao, X., & Ferreira, L. G. (2002). Overview of the radiometric and biophysical performance of the MODIS vegetation indices. *Remote Sensing of Environment*, *83*(1–2), 195–213. https://doi.org/10.1016/s0034-4257(02)00096-2

Huete, A., Liu, H. Q., Batchily, K., & Van Leeuwen, W. (1997). A comparison of vegetation indices over a global set of TM images for EOS-MODIS. *Remote Sensing of Environment*, *59*, 440–451. https://doi.org/10.1016/S0034-4257(96)00112-5

Izaurralde, R. C., Malhi, S. S., Nyborg, M., Solberg, E. D., & Quiroga Jakas, M. C. (2006). Crop performance and soil properties in two artificially eroded soils in north-central Alberta. *Agronomy Journal*, *98*(5), 1298–1311. https://doi.org/10.2134/agronj2005.0184.

IUSS Working Group WRB. (2015). *World Reference Base for Soil Resources 2014, update 2015. International soil classification system for naming soils and creating legends for soil maps*. World Soil Resources Reports No. 106. Rome: FAO.

Jin, X., Li, Z., Yang, G., Yang, H., Feng, H., Xu, X., … Luo, J. (2017). Winter wheat yield estimation based on multi-source medium resolution optical and radar imaging data and the AquaCrop model using the particle swarm optimization algorithm. *ISPRS Journal of Photogrammetry and Remote Sensing*, *126*, 24–37. https://doi.org/10.1016/j.isprsjprs.2017.02.001

Jin, X., Yang, G., Xu, X., Yang, H., Feng, H., Li, Z., … Zhao, C. (2015). Combined multi-temporal optical and radar parameters for estimating LAI and biomass in winter wheat using HJ and RADARSAR-2 data. *Remote Sensing*, *7*(10), 13251–13272. https://doi.org/10.3390/rs71013251

Kappler, C., Kaiser, K., Tanski, P., Klos, F., Fülling, A., Mrotzek, A., … Bens, O. (2018). Stratigraphy and age of colluvial deposits indicating late Holocene soil erosion in northeastern Germany. *Catena*, *170*, 224–245. https://doi.org/10.1016/j.catena.2018.06.010

Kaspar, T. C., Pulido, D. J., Fenton, T. E., Colvin, T. S., Karlen, D. L., Jaynes, D. B., & Meek, D. W. (2004). Relationship of corn and soybean yield to soil and terrain properties. *Agronomy Journal*, *96*(3), 700–709. https://doi.org/10.2134/agronj2004.0700

Keller, T., Sandin, M., Colombi, T., Horn, R., & Or, D. (2019). Historical increase in agricultural machinery weights enhanced soil stress levels and adversely affected soil functioning. *Soil and Tillage Research*, *194*, 104293. https://doi.org/10.1016/j.still.2019.104293

Kim, H. O., & Yeom, J. M. (2012). Multi-temporal spectral analysis of rice fields in South Korea using MODIS and RapidEye satellite imagery. *Journal of Astronomy and Space Sciences*, *29*(4), 407–411. https://doi.org/10.5140/jass.2012.29.4.407

Koszinski, S., Gerke, H. H., Hierold, W., & Sommer, M. (2013). Geophysical-based modeling of a kettle hole catchment of the morainic soil landscape. *Vadose Zone Journal*, *12*(4), 1–18. https://doi.org/10.2136/vzj2013.02.0044

Kravchenko, A. N., Robertson, G. P., Thelen, K. D., & Harwood, R. R. (2005). Management, topographical, and weather effects of spatial variability of crop grain yields. *Agronomy Journal*, *97*, 514–523. https://doi.org/10.2134/agronj2005.0514

Lal, R., Ahmadi, M., & Bajracharya, R. M. (2000). Erosional impacts on soil properties and corn yield on Alfisols in Central Ohio. *Land Degradation & Development*, *11*, 575–585. https://doi.org/10.1002/1099-145X(200011/12)11:6<575::AID-LDR410>3.0.CO;2-N

Lal, R., Mokma, D., & Lowery, B. (1999). Relation between soil quality and erosion. In R. Lal (Ed.), *Soil quality and soil erosion* (pp. 237–258). Boca Raton, FL: CRC Press.

Landesamt für Umwelt, Gesundheit und Verbraucherschutz Brandenburg, & Landesvermessung und Geobasisinformation Brandenburg. (2012). *Digital elevation model with a grid size of 1 m (DEM1) derived from laser scan data*. Potsdam, Germany: Landesamt.

Larney, F. J., Janzen, H. H., Olson, B. M., & Olson, A. F. (2009). Erosion-productivity-soil amendment relationships for wheat over 16 years. *Soil and Tillage Research*, *103*(1), 73–83. https://doi.org/10.1016/j.still.2008.09.008

Li, Y., Frielinghaus, M., Bork, H. R., Friedland, E. M., Schkade, U. K., Naumann, M., & Schäfer, H. (2002). Slope basis deposits linked to long-term land use in NE-Germany. *Archives of Agronomy and Soil Science*, *48*(4), 335–342. https://doi.org/10.1080/03650340214199

Lischeid, G., Balla, D., Dannowski, R., Dietrich, O., Kalettka, T., Merz, C., … Steidl, J. (2017). Forensic hydrology: What function tells about structure in complex settings. *Environmental Earth Sciences*, *76*(40), 1–15. https://doi.org/10.1007/s12665-016-6351-5

Lobb, D. A., Kachanoski, R. G., & Miller, M. H. (1995). Tillage translocation and tillage erosion on shoulder slope landscape positions measured

using Cs-137 as a tracer. *Canadian Journal of Soil Science*, *75*(2), 211–218. https://doi.org/10.4141/cjss95-029

Lüthgens, C., Böse, M., & Preusser, F. (2011). Age of the Pomeranian ice-marginal position in northeastern Germany determined by optically stimulated luminescence (OSL) dating of glaciofluvial sediments. *Boreas*, *40*(4), 598–615. https://doi.org/10.1111/j.1502-3885.2011.00211.x

Martinez-Feria, R. A., & Basso, B. (2020). Unstable crop yields reveal opportunities for site-specific adaptations to climate variability. *Scientific Reports*, *10*(1), 2885. https://doi.org/10.1038/s41598-020-59494-2

Matsushita, B., Yang, W., Chen, J., Onda, Y., & Qiu, G. Y. (2007). Sensitivity of the enhanced vegetation index (EVI) and normalized difference vegetation index (NDVI) to topographic effects: A case study in high-density cypress forest. *Sensors*, *7*(11), 2636–2651. https://doi.org/10.3390/s7112636

Moulin, A. P., Anderson, D. W., & Mellinger, M. (1994). Spatial variability of wheat yield, soil properties and erosion in hummocky terrain. *Canadian Journal of Soil Science*, *74*(2), 219–228. https://doi.org/10.4141/cjss94-030

Olson, K. R., Gennadiyev, A. N., Jones, R. L., & Chernyanskii, S. (2002). Erosion patterns on cultivated and reforested hillslopes in Moscow region, Russia. *Soil Science Society of America Journal*, *66*(1), 193–201. https://doi.org/10.2136/sssaj2002.1930a

Papiernik, S. K., Lindstrom, M. J., Schumacher, J. A., Farenhorst, A., Stephens, K. D., Schumacher, T. E., & Lobb, D. A. (2005). Variation in soil properties and crop yield across an eroded prairie landscape. *Journal of Soil and Water Conservation*, *60*(6), 388–395.

Peichl, M., Thober, S., Meyer, V., & Samaniego, L. (2018). The effect of soil moisture anomalies on maize yield in Germany. *Natural Hazards and Earth System Sciences*, *18*(3), 889–906. https://doi.org/10.5194/nhess-18-889-2018

Pennock, D. J. (2003). Terrain attributes, landform segmentation, and soil redistribution. *Soil & Tillage Research*, *69*(1–2), 15–26. https://doi.org/10.1016/S0167-1987(02)00125-3

Planet Team. (2016). *RapidEye imagery product specifications. Version 6.1*. San Francisco, CA, USA: Planet.

Quinton, J. N., Govers, G., Van Oost, K., & Bardgett, R. D. (2010). The impact of agricultural soil erosion on biogeochemical cycling. *Nature Geoscience*, *3*(5), 311–314. https://doi.org/10.1038/ngeo838

Reichenau, T. G., Korres, W., Montzka, C., Fiener, P., Wilken, F., Stadler, A., … Schneider, K. (2016). Spatial heterogeneity of leaf area index (LAI) and its temporal course on arable land: Combining field measurements, remote sensing and simulation in a comprehensive data analysis approach (CDAA). *PLoS One*, *11*(7), e0158451. https://doi.org/10.1371/journal.pone.0158451

Renard, K. G., Foster, G. R., Weesies, G. A., McCool, D. K., & Yoder, D. C. (1997). *Predicting soil erosion by water: A guide to conservation planning with the revised universal soil loss equation (RUSLE): Agriculture Handbook 703*. Washington, DC: USDA-ARS.

Rudolph, S., van der Kruk, J., von Hebel, C., Ali, M., Herbst, M., Montzka, C., … Weihermüller, L. (2015). Linking satellite derived LAI patterns with subsoil heterogeneity using large-scale ground-based electromagnetic induction measurements. *Geoderma*, *241-242*, 262–271. https://doi.org/10.1016/j.geoderma.2014.11.015

Schimmack, W., Auerswald, K., & Bunzl, K. (2002). Estimation of soil erosion and deposition rates at an agricultural site in Bavaria, Germany, as derived from fallout radiocesium and plutonium as tracers. *Naturwissenschaften*, *89*(1), 43–46. https://doi.org/10.1007/s00114-001-0281-z

Schwertmann, U., Vogl, W., & Kainz, M. (1987). *Bodenerosion durch Wasser. Vorhersage des Bodenabtrags und Bewertung von Gegenmaßnahmen*. Stuttgart: Ulmer Verlag.

Shang, J., Liu, J., Huffman, T., Qian, B., Pattey, E., Wang, J., … Lantz, N. (2014). Estimating plant area index for monitoring crop growth dynamics using Landsat-8 and RapidEye images. *Journal of Applied Remote Sensing*, *8*(1), 085196. https://doi.org/10.1117/1.Jrs.8.085196

Shang, J., Liu, J., Ma, B., Zhao, T., Jiao, X., Geng, X., … Walters, D. (2015). Mapping spatial variability of crop growth conditions using RapidEye data in northern Ontario, Canada. *Remote Sensing of Environment*, *168*, 113–125. https://doi.org/10.1016/j.rse.2015.06.024

Singh, K., Choudhary, O. P., Singh, H. P., Singh, A., & Mishra, S. K. (2019). Sub-soiling improves productivity and economic returns of cotton-wheat cropping system. *Soil and Tillage Research*, *189*, 131–139. https://doi.org/10.1016/j.still.2019.01.013

Sommer, M., Fiedler, S., Glatzel, S., & Kleber, M. (2004). First estimates of regional (Allgäu, Germany) and global CH_4 fluxes from wet colluvial margins of closed depressions in glacial drift areas. *Agriculture, Ecosystems & Environment*, *103*(1), 251–257. https://doi.org/10.1016/j.agee.2003.09.019

Sommer, M., Gerke, H. H., & Deumlich, D. (2008). Modelling soil landscape genesis. A "time split" approach for hummocky agricultural landscapes. *Geoderma*, *145*(3–4), 480–493. https://doi.org/10.1016/j.geoderma.2008.01.012

Stadler, A., Rudolph, S., Kupisch, M., Langensiepen, M., van der Kruk, J., & Ewert, F. (2015). Quantifying the effects of soil variability on crop growth using apparent soil electrical conductivity measurements. *European Journal of Agronomy*, *64*, 8–20. https://doi.org/10.1016/j.eja.2014.12.004

Stone, J. R., Gilliam, J. W., Cassel, D. K., Daniels, R. B., Nelson, L. A., & Kleiss, H. J. (1985). Effect of erosion and landscape position on the productivity of Piedmont soils. *Soil Science Society of America Journal*, *49*, 987–991. https://doi.org/10.2136/sssaj1985.03615995004900040039x

Sui, Y., Liu, X., Jin, J., Zhang, S., Zhang, X., Herbert, S. J., & Ding, G. (2009). Differentiating the early impacts of topsoil removal and soil amendments on crop performance/productivity of corn and soybean in eroded farmland of Chinese Mollisols. *Field Crops Research*, *111*(3), 276–293. https://doi.org/10.1016/j.fcr.2009.01.005.

Taylor, J. C., Wood, G. A., Earl, R., & Godwin, R. J. (2003). Soil factors and their influence on within-field crop variability, part II: Spatial analysis and determination of management zones. *Biosystems Engineering*, *84*(4), 441–453. https://doi.org/10.1016/s1537-5110(03)00005-9

Thaler, E. A., Larsen, I. J., & Yu, Q. (2021). The extent of soil loss across the US Corn Belt. *Proceedings of the National Academy of Sciences of the United States of America*, *118*(8), e1922375118. https://doi.org/10.1073/pnas.1922375118

Thorup-Kristensen, K., Salmerón Cortasa, M., & Loges, R. (2009). Winter wheat roots grow twice as deep as spring wheat roots, is this important for N uptake and N leaching losses? *Plant and Soil*, *322*(1–2), 101–114. https://doi.org/10.1007/s11104-009-9898-z

Tso, B., & Mather, P. (2009). *Classification methods for remotely sensed data* (Vol. 2). Boca Raton, FL: CRC Press.

Van der Meij, W. M., Reimann, T., Vornehm, V. K., Temme, A. J. A. M., Wallinga, J., Beek, R., & Sommer, M. (2019). Reconstructing rates and patterns of colluvial soil redistribution in agrarian (hummocky) landscapes. *Earth Surface Processes and Landforms*, *44*, 2408–2422. https://doi.org/10.1002/esp.4671

Van Oost, K., Govers, G., De Alba, S., & Quine, T. A. (2006). Tillage erosion: A review of controlling factors and implications for soil quality. *Progress in Physical Geography*, *30*(4), 443–466. https://doi.org/10.1191/0309133306pp487ra

Van Oost, K., Govers, G., & Desmet, P. (2000). Evaluating the effects of changes in landscape structure on soil erosion by water and tillage. *Landscape Ecology*, *15*, 577–589. https://doi.org/10.1023/A:1008198215674

Van Oost, K., Quine, T. A., Govers, G., & Heckrath, G. (2006). Modeling soil erosion induced carbon fluxes between soil and atmosphere on

agricultural land using SPEROS-C. In E. J. Roose, R. Lal, C. Feller, B. Barthes, & B. A. Stewart (Eds.), *Advances in soil science. Soil erosion and carbon dynamics*, (37–51). Boca Raton, FL: CRS Press.

Vogel, E., Deumlich, D., & Kaupenjohann, M. (2016). Bioenergy maize and soil erosion-risk assessment and erosion control concepts. *Geoderma*, *261*, 80–92. https://doi.org/10.1016/j.geoderma.2015.06.020

Wehrhan, M., Rauneker, P., & Sommer, M. (2016). UAV-based estimation of carbon exports from heterogeneous soil landscapes. A case study from the CarboZALF experimental area. *Sensors*, *16*(2), 255. https://doi.org/10.3390/s16020255

Wilken, F., Baur, M., Sommer, M., Deumlich, D., Bens, O., & Fiener, P. (2018). Uncertainties in rainfall kinetic energy-intensity relations for soil erosion modelling. *Catena*, *171*, 234–244. https://doi.org/10.1016/j.catena.2018.07.002

Wilken, F., Ketterer, M., Koszinski, S., Sommer, M., & Fiener, P. (2020). Understanding the role of water and tillage erosion from $^{239+240}$Pu tracer measurements using inverse modelling. *The Soil*, *6*, 549–564. https://doi.org/10.5194/soil-6-549-2020

Wilken, F., Sommer, M., Van Oost, K., Bens, O., & Fiener, P. (2017). Process-oriented modelling to identify main drivers of erosion-induced carbon fluxes. *The Soil*, *3*(2), 83–94. https://doi.org/10.5194/soil-3-83-2017

Zhao, P., Li, S., Wang, E., Chen, X., Deng, J., & Zhao, Y. (2018). Tillage erosion and its effect on spatial variations of soil organic carbon in the black soil region of China. *Soil and Tillage Research*, *178*, 72–81. https://doi.org/10.1016/j.still.2017.12.022

How to cite this article: Öttl, L. K., Wilken, F., Auerswald, K., Sommer, M., Wehrhan, M., & Fiener, P. (2021). Tillage erosion as an important driver of in-field biomass patterns in an intensively used hummocky landscape. *Land Degradation & Development*, 1–15. https://doi.org/10.1002/ldr.3968